Ten years of spectroscopic monitoring of the Yellow Hypergiant ρ Cas

C. Quandt[1], A. Lobel[2], S. Hold[3], G. Gebhard[4], D. Hutsemekers[5], J. Martin[6], T. Kremser[7], K. Vollmann[8]

Abstract

We present an analysis of ongoing optical spectroscopic monitoring of the Yellow Hypergiant Rho Cas between 2014 and 2024, with an observation cadence of 7 days since 2018. We discuss the temporal line profile variability observed in Balmer Hα and the variability of the stellar wind in selected photospheric absorption lines of Fe I and Si II. We combine accurate measurements of various line parameters with multi-band photometric observations during this period and present an analysis of the pulsation periods in this notorious hypergiant star.

1. Introduction

Yellow hypergiants such as ρ Cas (Ia$^+$), represent an important evolutionary stage of the most massive stars between cool red SGs and hot SGs, near the end of their lives (Kraus et al. 2019; Lobel et al. 2003). Despite extensive research many properties of these evolved stars remain currently unclear. We aim to investigate the variable stellar parameters and pulsation behaviour of Rho Cas from a long-term spectroscopic monitoring campaign with an about weekly cadence since July 2018.

2. Observations and calibration

- 352 long-slit and echelle spectra observed between 2014 and 2024, with a cadence $\sim$7 days since July 2018.
- $\lambda\lambda$ 6330 to 6600 Å with spectral resolving power R = 10,000 to 20,000.
- Telescope apertures of 5" to 16" + 1.2m TIGRE for observing long-slit and echelle spectra.
- ESO-MIDAS pipeline calibration processing, including automated continuum flux normalization.
- Analysis of line equivalent widths, FWHM, bi-sector, and absorption line depths for spectroscopic Teff measurements and Lomb-Scargle period determination.

3. Dynamic line spectra since 2018

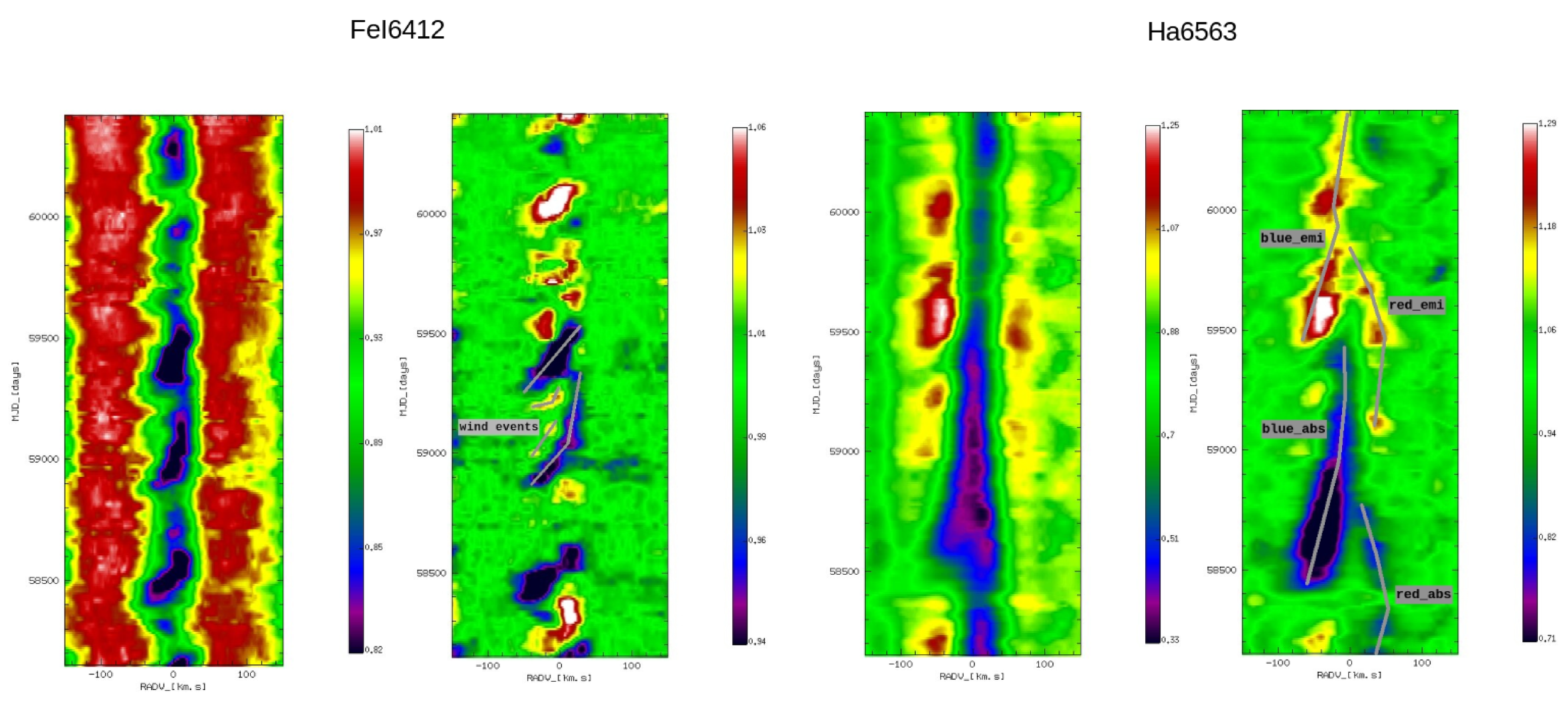

First from left: Dynamic spectrum of the photospheric Fe I λ6412 line in the stellar rest frame (time runs upwards). The central line depth varies quasi-periodically with time. We observe prominent flux variability in the short-wavelength line wing caused by variable wind opacity, combined with changes of the normalized line depth. **Second from left:** Residual dynamic spectrum of Fe I λ6412 (normalized line flux minus the time-averaged line flux). Notice the wind events occurring between MJD 58800 and 59600. The violet line wing becomes more extended and next weakens, followed by a gradual red-shift in the central line core. **Third from left:** Dynamic spectrum of the Balmer Hα line. Notice the prominent wind event around MJD 58500 revealing strongly enhanced wind absorption. **Fourth from left:** Residual dynamic Hα spectrum showing changes from line wing absorption into emission. The violet Hα line wing is in absorption around MJD 58500 and fades away over $\sim$500 d. It reveals strong emission around MJD 59400 while the inverse Hα P Cyg line profile fades away over the next two years. We also observe weak absorption and emission flux variability in the long-wavelength Hα line wing. We find Hα line profile variability of at least twice longer compared to the photospheric Fe I lines.

4. Lomb-Scargle period analysis of 4 years

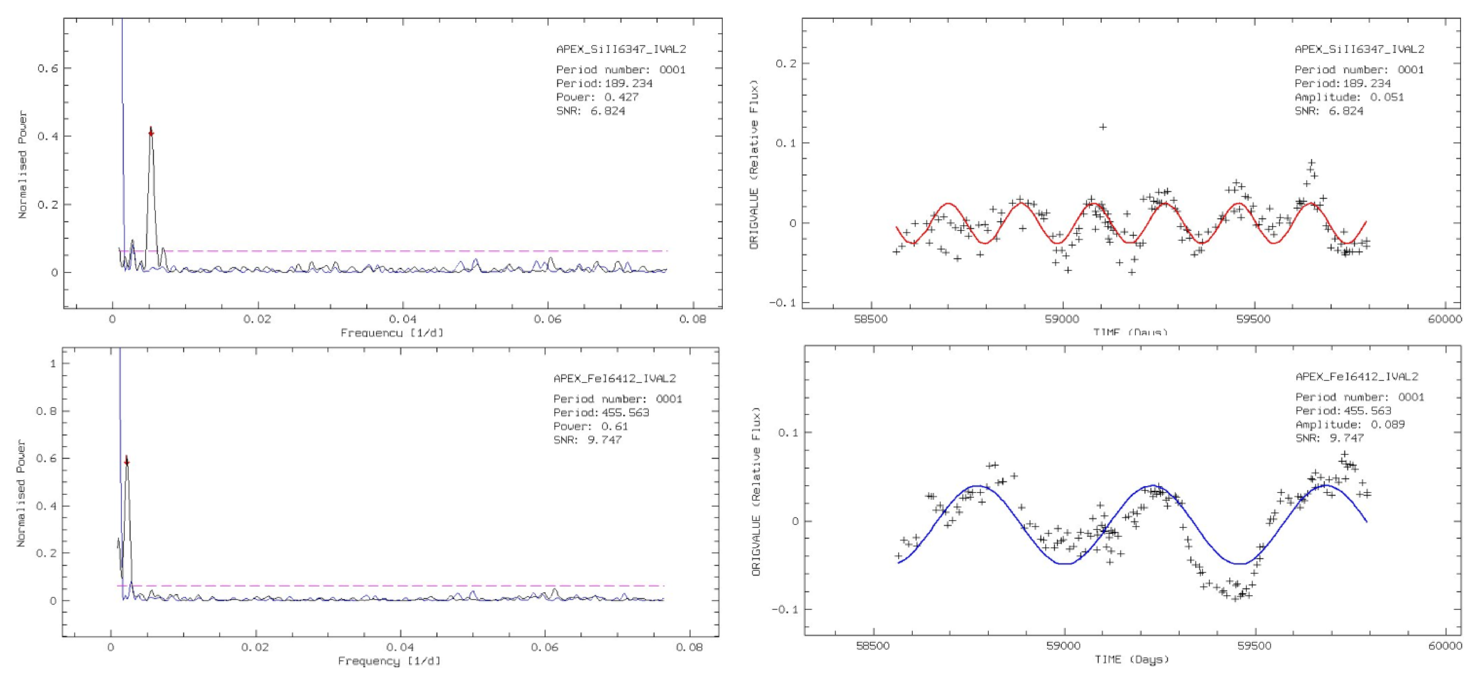

Top left and right: Periodogram and model from a Lomb-Scargle analysis of the variable ionic Si II λ6347 normalized absorption line depth. We find a pulsation period of 189 d over a time interval of four years (red drawn sine curve). **Bottom left and right:** Periodogram and model from a Lomb-Scargle analysis of the variable Fe I λ6412 normalized absorption line depth. We find a variability period of 456 d (blue sine curve).

9. Addresses and Acknowledgements

[1] Schnörringen Telescope Science Institute, D-51545 Waldbröl, Germany; E-mail: christoph.quandt@gmail.com
[2] Royal Observatory of Belgium, Ringlaan 3, B-1180 Brussels, Belgium
[3] Sternwarte Schulberg, A-8323 St.Marein, Austria
[4] Ohmstraße 9, D-92318 Neumarkt, Germany
[5] FNRS, University of Liège, Belgium
[6] Huggins Spectroscopic Observatory, UK
[7] Rollsdorf, A-153 8181 St. Ruprecht, Austria
[8] Schnörringen Telescope Science Institute, D-51545 Waldbröl, Germany; E-mail: klaus.vollmann@stsci.de

A.L. acknowledges in part funding from the European Union's Framework Programme for Research and Innovation Horizon 2020 (2014-2020) under the Marie Skłodowska-Curie grant Agreement No. 823734: Physics of Extreme Massive Stars (EC-POEMS). We acknowledge with thanks the variable star observations from the AAVSO International Database contributed by observers worldwide and used in this research. The spectra of the calibration stars, used to establish the Teff-LDR relationships, come from spectra retrieved from the ELODIE archive at Observatoire de Haute-Provence (OHP, http://atlas.obs-hp.fr/elodie/) and ESO Science Archive Facility (http://archive.eso.org/cms.html). This work has made use of data from the European Space Agency (ESA) mission *Gaia* (`https://www.cosmos.esa.int/gaia`), processed by the *Gaia* Data Processing and Analysis Consortium (DPAC, `https://www.cosmos.esa.int/web/gaia/dpac/consortium`). Funding for the DPAC has been provided by national institutions, in particular the institutions participating in the *Gaia* Multilateral Agreement.

5. Spectroscopic Teff from photospheric line depth ratios

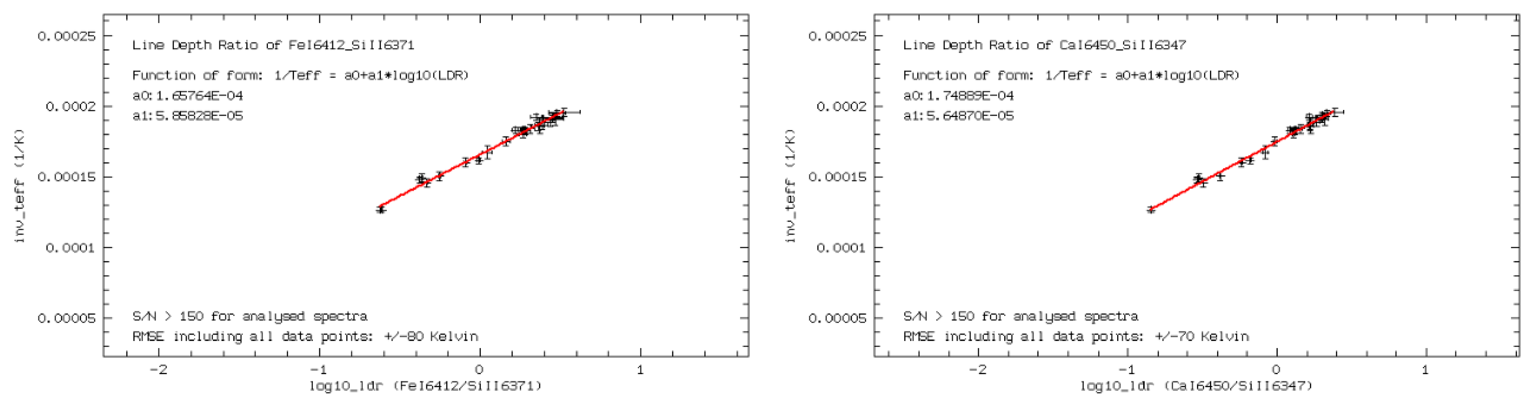

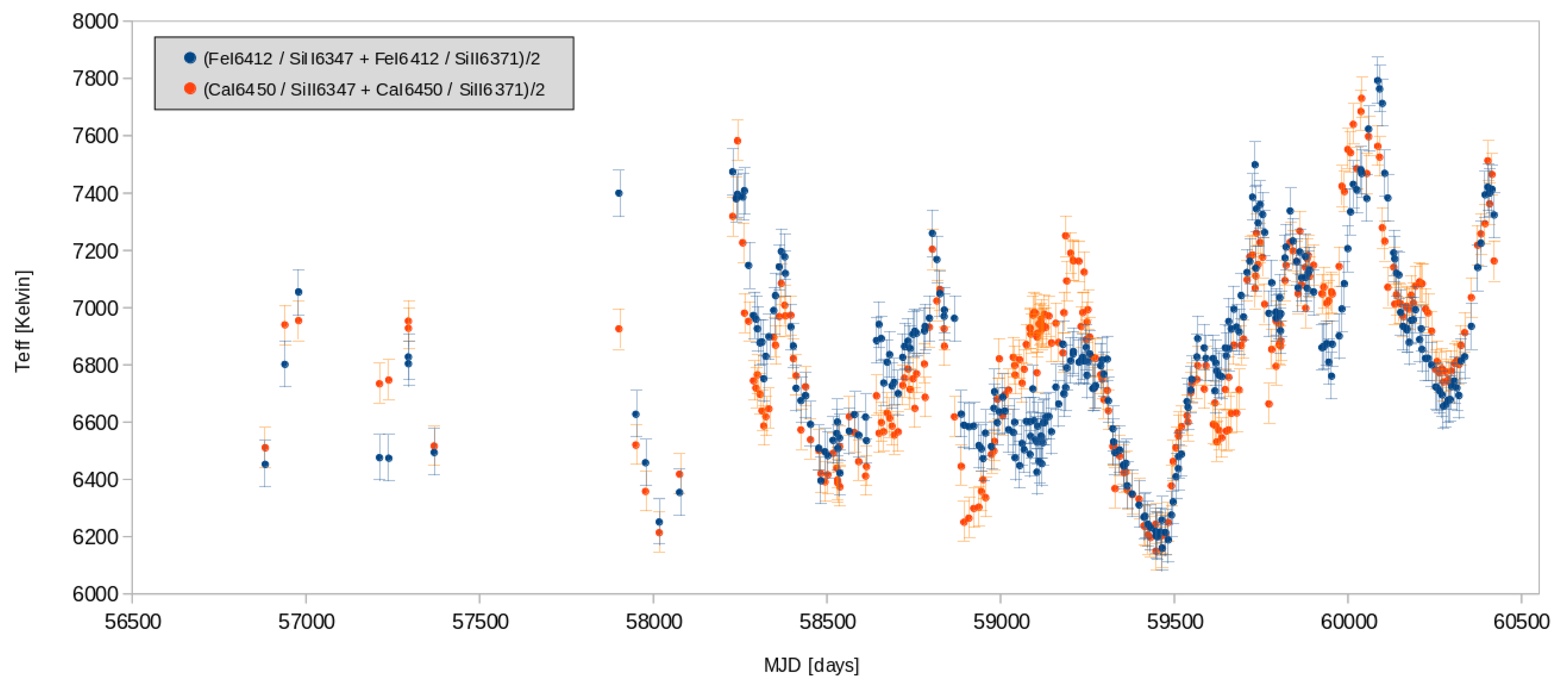

Top panels: Calibration plots of selected line depth ratios (LDRs) for determining the stellar effective temperature Teff. The calibrations are derived from a sample of AFGK supergiants using known effective temperatures from Kovtyukh (2007) and Gaia DR3. The spectra for obtaining the LDRs are taken from the ELODIE database and the ESO Science Archive Facility. **Bottom panel:** Spectroscopic Teff-values calculated using two LDRs for two different neutral photospheric metal lines of Fe I λ6412 and Ca I λ6450. For the time interval around MJD 59100, we find a best match within an estimated errorbar of $\pm$80 K. Around MJD 59100, however, we find a maximum Teff-difference of $\sim$500 K between both lines. We determine Teff-values ranging from 6200 K to 7800 K from continuous spectroscopic monitoring since July 2018.)

6. Comparison of spectroscopy and broad-band photometry

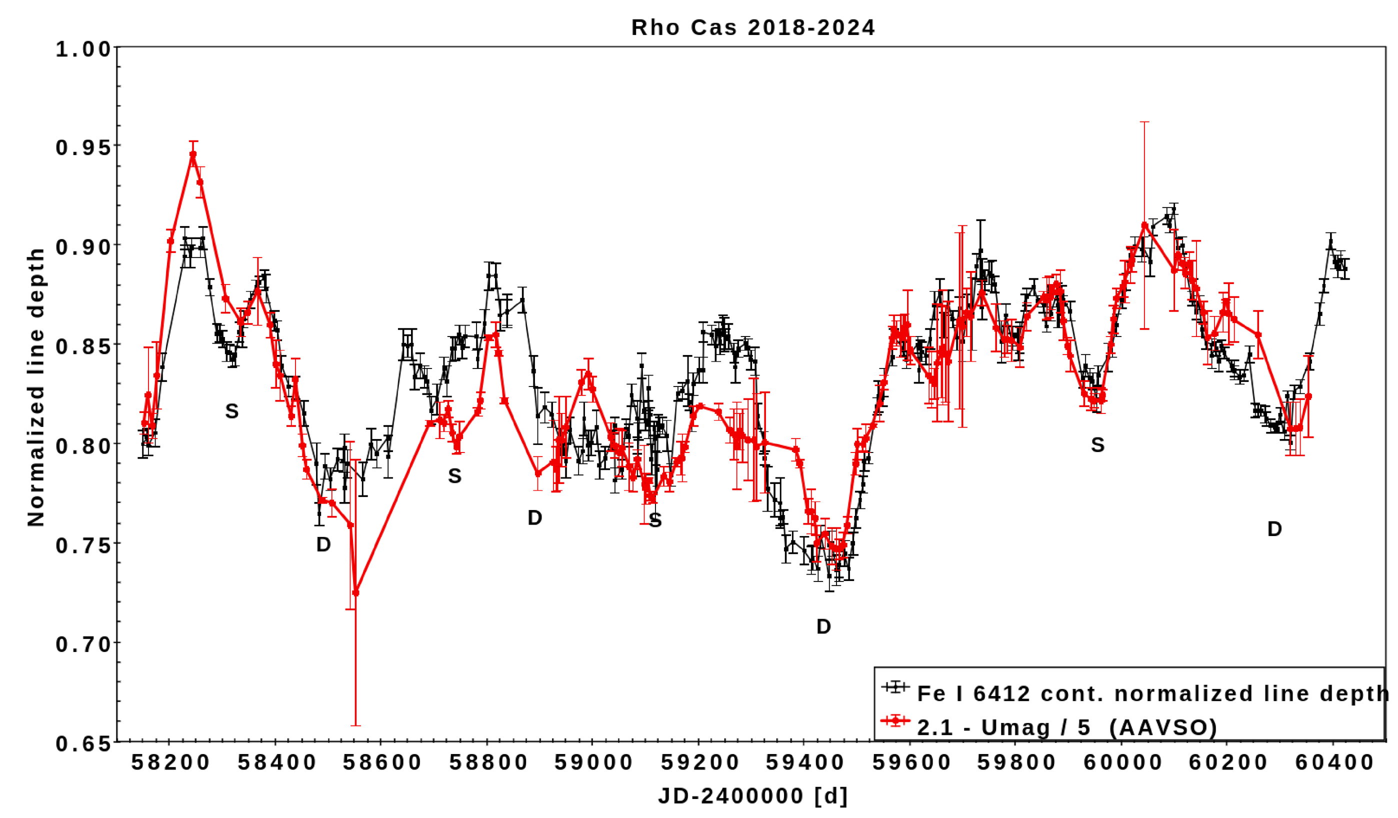

Figure caption: Photospheric Fe I λ6412 continuum normalized line depths (black symbols) observed in 2018-2024 compared to U-band magnitude observations from AAVSO (red symbols). We find good correspondence between the variable Fe I line depths and the (scaled) U-magnitudes, signaling that our continuum flux normalization procedures are sufficiently accurate for reliable Teff measurements and LS period determinations in 4. and 5. We find good overall correspondence between both curves within the assigned errorbars, including the short-term variability in both curves. We observe similar agreement between the variable depths of other photospheric metal lines and the AAVSO UBV-band brightness curves. The correlation between the photospheric line depths and the broad-band continuum fluxes is caused by the variable Teff (and logg) during the quasi-periodical oscillations of the yellow hypergiant's extended atmosphere. Notice also the remarkable alternating shallow (marked S) and deep (D) U-brightness minima, repeating four times in 2018-2024, reminiscent of the brightness variability typically observed in lesser massive pulsating RV Tau stars.

7. Conclusions

- The dynamic spectra of the Fe I λ6412 and Balmer Hα lines show different behaviour with time in part due to wind events. We find a frequent occurrence of emission in the Hα line wings from MJD 59500 that is correlated with larger Teff over the quasi-periodic pulsations of ρ Cas.
- Our Lomb-Scargle analysis of the Si II λ6347 absorption line depth variability reveals a dominant period of $\simeq$189 days. The Fe I λ6412 line depth variability shows a longer period of 456 d.
- The spectroscopic Teff-values we measure from the metal line depth ratios are in agreement within errorbars of ±80 K. For certain time intervals, however, we calculate differences of $\sim$500 K between both photospheric ionic lines. These large Teff-deviations correlate with wind events in which the violet line wings extend further due to enhanced wind opacity.
- We find Hα line profile variability of at least twice longer compared to the photospheric metal absorption lines.
- We find good correlation between variable Fe I line depths and broad-band U-magnitudes, signaling that our continuum flux normalization procedures are accurate for reliable Teff measurements and LS period determinations.

8. References

Kraus, M., Kolka, I., Aret, A., et al. 2019, MNRAS, 483, 379
Lobel, A. et al. 2003, ApJ, 583, 923; alobel.freeshell.org/rcas.html
Kovtyukh, V. V., 2007, MNRAS, 378, 617624